J Mater Sci (2008) 43:1802–1810
DOI 10.1007/s10853-007-2342-y

# Activation energy for growth in single size distribution and the dissolution features of $\gamma'$ precipitates in the superalloy IN738LC

**A. K. Dwarapureddy · E. Balikci · S. Ibekwe · A. Raman**

Received: 26 April 2007 / Accepted: 27 November 2007 / Published online: 18 January 2008


**Abstract** Activation energy for the growth of $\gamma'$ precipitates in single size unimodal distribution has been determined by annealing the solution-treated and quenched alloy with fine 70 nm size cooling precipitates at 1,040°, 1,080°, and 1,100 °C for different periods of time up to 100 h. Results obtained using the LSW matrix diffusion model concur with the deductions of earlier work that the activation energy for growth of precipitates in single size distribution is not a constant, but increases with increasing size of precipitates. Also, the activation energy plotted against the corresponding precipitate sizes yields a straight line with a positive slope. During long-time annealing, precipitate particles line up to reduce interactive free energy and grow to fairly coarse sizes along the matrix grain boundaries. Some of the particles in isolated islands or those lined along the matrix grain boundaries attain critical maximum sizes and begin to dissolve into the matrix in four different ways, designated as Modes 1 through 4. The various modes of dissolution are described and the possibility of repeated growth and dissolution in cycles is envisaged.

A. K. Dwarapureddy · A. Raman (✉)
Materials Group, Mechanical Engineering Department,
Louisiana State University, Baton Rouge, LA 70803, USA
e-mail: meraman@me.lsu.edu

E. Balikci
Department of Mechanical Engineering,
Bogazici University - South Campus, Bebek,
Istanbul, Turkey

S. Ibekwe
Mechanical Engineering Department, Southern University,
Baton Rouge, LA 70813, USA

## Introduction

The Ni-based superalloy IN738LC with the $\gamma'$ precipitates in the duplex size (coarse and fine) distribution in the solid solution matrix is in use for selected gas turbine components. Single size distribution of extremely fine precipitate particles is obtainable after an initial solution-treating heat treatment, followed by quenching in water [1, 2]. The fine precipitate particles grow when the alloy is heated and maintained at high temperatures. Features of their growth and the corresponding activation energy have been studied in the temperature range 850–1,120 °C by annealing the alloy with fine cooling precipitates (produced by heating the alloy first at 1,200 °C and quenching thereafter in water) at different temperatures for 25 h [1, 2]. The study showed that with increasing temperature and with the corresponding increased size in the nearly single size (unimodal) precipitate distribution, the activation energy for their growth seemed to have progressively increased. However, a later study of precipitate growth features in the duplex size (mixed coarse and fine) precipitate distribution (obtained by solution treating at 1,200 °C first and, subsequently, heating the alloy for a few hours in the precipitate partial dissolution zone (1,130–1,150 °C) at 1,140 °C, and water quenching; or by water quenching from 1,200 °C, reheating at 1,120 °C for 24 h to get single size coarse precipitates, then heating in the precipitate partial dissolution zone at 1,140 °C for a few hours and water quenching thereafter to produce secondary fine cooling precipitates) at high temperatures below the precipitate partial dissolution zone, indicated that the activation energies for the growth of both the fine and coarse precipitates in the duplex size distribution decrease with their increasing size [3]. The latter study was undertaken by heating the duplex precipitated alloy for different

times at three different high temperatures in the range 980–1,100 °C. This anomalous behavior, different from the requirements for growth of single size precipitates, as well as the lack of more precise data for the single size precipitate distribution at such high temperatures prompted the authors to revisit this topic and study more critically the growth features of the $\gamma'$ precipitates at similar high temperatures when heated for various lengths of time. Another concurrent topic of interest was to determine if there is a largest size that can be reckoned as the critical size to which the single size particles would grow and study processes, if any, that would take place subsequently. From earlier analysis and deductions, three scenarios could be projected.

(i) The size stays at the coarsest level forever at the given temperature.
(ii) The coarsest precipitate splits into two [4, 5] or eight fragments [5, 6] after reaching some critical size [7].
(iii) The coarsest particle begins to dissolve in the matrix, either after splitting into fragments or through direct dissolution starting from the interface [8] or from its center [4, 9].

The current study focuses on the above given issues and uses similar procedures as in prior investigations from the group [1–3].

## Experimental

Thin slices of the cast alloy IN738LC, cut from the as-received, supplier heat-treated bars [1, 2] (composition: Ni—16%Cr, 8.35%Co, 1.61%Mo, 2.52%W, 1.74%Ta, 0.71%Nb, 3.5%Al, 3.32%Ti, 0.03%Zr, 0.03%Si, 0.011%B, 0.09%C) were wrapped in stainless steel foils, sealed in vacuum in quartz glass tubes, and solution-treated and water-quenched (1,200 °C—4 h/WQ) to obtain single size cooling precipitates of average size ~70 nm. After this treatment, individual pieces were sealed in vacuum in separate quartz tubes and annealed at 1,040°, 1,080°, and 1,100 °C for the time periods of 3, 13, 25, 50, 75, 100, 125, 150, 175, and 200 h. After the specified time periods at the above given temperatures, the capsules were removed from the furnace, one corresponding to each case, and quenched in cold water. Cold water quenching was to retain the precipitate size, the same as at the annealing temperature prior to quenching.

For microstructure analysis, the ground and polished samples were etched with a solution of 33% $HNO_3$ + 33% acetic acid + 33% water + 1% HF. Hitachi 2460 and S-3660N scanning electron microscopes were used to study the morphology and sizes of precipitate particles. For precipitate size evaluations and comparisons, the magnification was maintained at 5k× in all cases. Suitable other magnifications were used to study other related features observed in the microstructures.

Precipitate size measurements were carried out on the SEM-generated microstructure images using the SCION IMAGE software of Scion Corporation, Inc. Reported sizes were obtained after measuring the average sizes of as many particles as possible, usually around 100. From the microstructure observations, it was determined that annealing the quenched alloy with cooling precipitates up to 100 h retained their near-single size unimodal distribution, whereas for periods over 100 h at 1,080° and 1,100 °C some of the particles, particularly located along the matrix grain boundaries, started to coarsen faster, resulting in segregated duplex size distribution for the precipitate. Hence, in order to evaluate the growth activation energies in single size distribution of precipitates their sizes after the various time periods of annealing only up to 100 h at the three temperatures mentioned above were utilized. Sizes of individual coarsened particles along grain boundaries were measured likewise and recorded in cases where critical coarsest sizes were deemed to be approaching or have been attained.

## Results and discussion

### Precipitate growth

As found already [1, 2], fine cooling precipitates of size about 70 nm were formed, Fig. 1a, after solution treating the as-received alloy (see Ref 2 for prior in-plant treatment of as-received cast rods) at 1,200 °C and water quenching. Subsequent annealing at 1,040°, 1,080°, and 1,100 °C for various time intervals led to gradual precipitate coarsening at these temperatures. The average precipitate sizes (diameter of approximately equivalent spheres), measured from the resultant microstructures, are given in Table 1. Some of the microstructures obtained after the annealing treatments at the chosen temperatures for selected time intervals are reproduced in Fig. 2. Growth rate is found to be slow at 1,040 °C, but it increases appreciably at 1,100 °C, as can be expected. Likewise, it is fast at the start at any given temperature, but tends to slow down as precipitates grow in size with increasing time.

Several distinct features of growth can be noticed. The precipitates retain their cuboidal shape until a fairly large size is reached. For example, the particles are still cuboidal, with a size of about 0.65 μm, even after 200 h of annealing at 1,040 °C, Fig. 2d-left. (They were likewise cuboidal with average size of about 700 nm after a 24 h anneal at 1,120 °C [1, 2].) They also are found to line up, forming rows of aligned particles. Such an alignment is obviously a

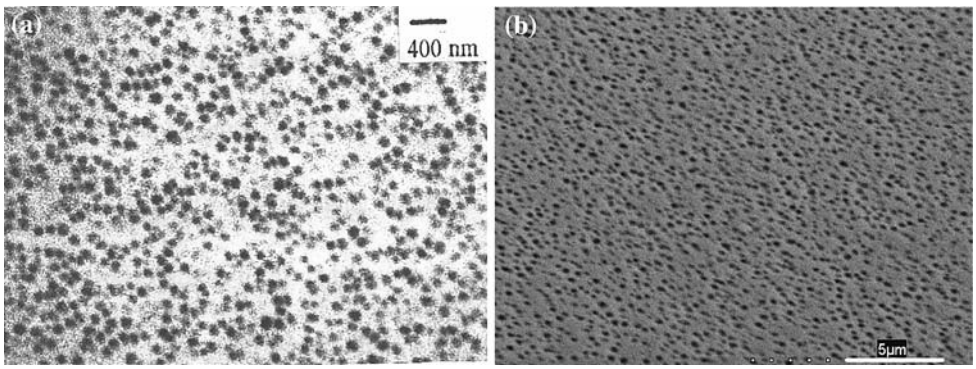


**Fig. 1** (**a**) Refined fine precipitate containing microstructure after 1,200 °C/4 h/WQ solution treatment (Magnification 15k×), Ref [1]. (**b**) Microstructure after 3 h annealing at 1,100 °C (Magnification 5k×), present work

**Table 1** Average precipitate size data in IN738LC samples annealed for various times at three different temperatures

| Annealing time (h) → Temp. (°C) ↓ | Average precipitate sizes (μm) | | | | | |
|---|---|---|---|---|---|---|
| | 3 | 13 | 25 | 50 | 75 | 100 |
| 1040 | 0.1879 ± 0.014 | 0.3052 ± 0.028 | 0.3656 ± 0.037 | 0.4369 ± 0.041 | 0.4523 ± 0.038 | 0.4860 ± 0.045 |
| 1080 | 0.2189 ± 0.0145 | 0.3651 ± 0.029 | 0.4404 ± 0.042 | 0.5811 ± 0.064 | 0.6357 ± 0.075 | 0.7523 ± 0.12 |
| 1100 | 0.2407 ± 0.014 | 0.4084 ± 0.029 | 0.5804 ± 0.068 | 0.6844 ± 0.12 | 0.7642 ± 0.135 | 0.8952 ± 0.136 |

prelude to their joining with each other to form rafts, and initial rafting at high temperatures tends to change them to slightly bulged, oval-shaped particles.

Concurrent with the change in morphology from cuboidal to oval, selected particles at favorable locations are found to have grown further, leading eventually to spheroidal morphology. The oval and spheroidal morphologies are apparent in the microstructures obtained after 50 h and 200 h at 1,100 °C, Fig. 2b-right and d-right. Large spheroidal particles are commonly found along the grain boundaries of the parent solid solution $\gamma$ phase. Selected microstructures containing such coarsened particles located along the matrix grain boundaries are given in Fig. 3.

The activation energy for the growth of precipitate particles is calculated using the equation given by the LSW theory [10, 11] for volume-based matrix diffusion of solute atoms [12].

$$d^n - d_0^n = kt \tag{1}$$

where

$$k = (8/9)\psi_{\text{int}}\Omega^2 D_{\text{T}} C_{\text{e}}/RT = 8/9\ [\psi_{\text{int}}\Omega^2 D_0 \exp\left(\frac{-Q}{RT}\right) C_{\text{e}}]/RT \tag{2}$$

($\psi_{\text{int}}$ = precipitate–matrix interfacial energy; $\Omega$ = molar volume of the precipitate phase; $D_0$ = diffusion constant; $Q$ = molar diffusion activation energy; $C_{\text{e}}$ = equilibrium solute concentration in the matrix phase; and $R$ = universal gas constant) which is approximated to:

$$k = k_0 \exp\left(\frac{-Q}{RT}\right) \tag{3}$$

The above first approximation implies that the variables such as $\psi_{\text{int}}$ and $C_{\text{e}}$ and any changes due to variation in the volume fraction $\varphi$ of the precipitate phase in the alloy are all included in $k_0$ and the RT in the denominator is absorbed into the Arrhenius term.

The growth exponent '$n$' was calculated from the data and verified to be close to three, and it is taken as three, as in our previous analysis [1, 2]. $Q$ in the above equation is taken as the molar activation energy for the precipitate growth process controlled by lattice diffusion (generally required to be a constant) and $d$ is the size (equivalent-sphere diameter) of the particles.

The alloy IN738LC has about 43 vol% of the $\gamma'$ precipitate phase and this remains nearly steady in the entire range of temperature up to the partial dissolution range, i.e., up to about 1,130 °C. Since the volume fraction of the precipitate phase remains nearly constant throughout and temperatures close to the solute dissolution temperature range are involved, it is assumed that the system is under the condition of steady ripening process. Also, unlike in the Ni–Al system, the matrix solid solution phase and the precipitate phase have compositions not widely different from each other, and the misfit is also very small, <0.5% [13]. The concentrations of the main solutes Al and Ti in the matrix ($C_{\text{e}}$) as well as in the precipitate phase appear to remain also nearly steady and any changes that could occur in the interface region may be neglected. Based on these conditions, it is assumed that $\psi_{\text{int}}$ remains nearly steady in the temperature range 1,040–1,100 °C and only the strain energy varies as the precipitates grow in size. It was felt that, as a first approximation, the $k_0$ term could be treated

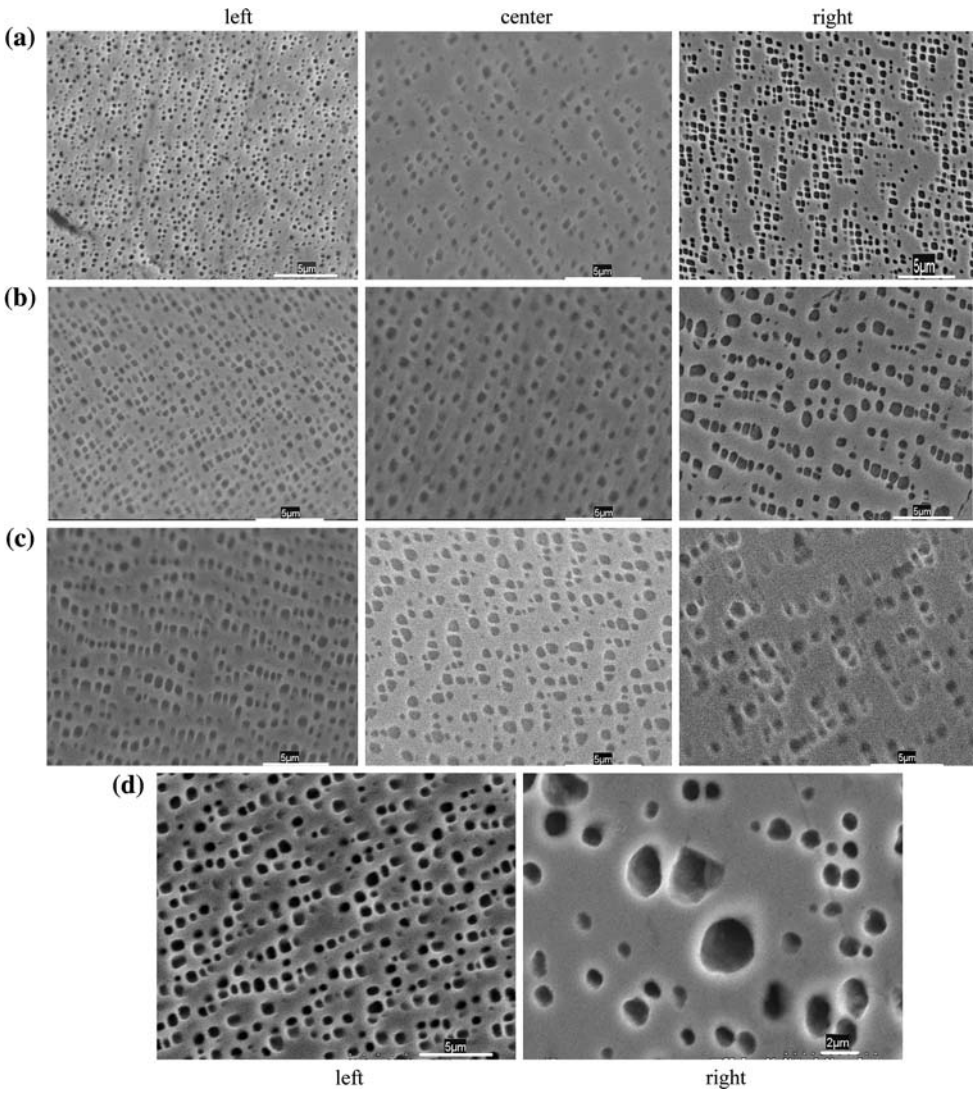


**Fig. 2** (**a**–**c**) Microstructures obtained after annealing at 1,040°, 1,080°, and 1,100 °C, respectively, after (**a**) 13 h (b) 50 h (c) 100 h, and (**d**) at 1,040° and 1,100 °C, respectively, after 200 h. Magnification: 5k×

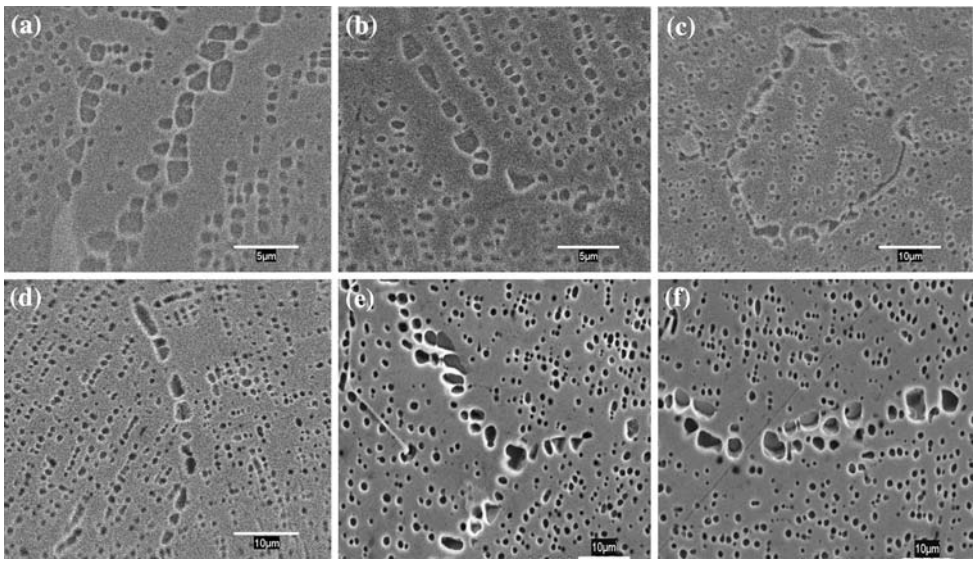


**Fig. 3** Microstructures after annealing at 1,100 °C for (**a**) 50 (**b**) 75 (**c**) 150, and (**d**, **e**, **f**) 200 h. Note different magnifications in (**a**) and (**b**) above, compared with the rest. Microstructures in (**d**), (**e**), and (**f**), and in Fig. 2d-right are at different locations. Magnification: 4k× (**a** and **b**); 2k× (**c**–**f**)

**Table 2** The '$Q$' and '$d$' values calculated for the mean temperatures 1,060, 1,070, and 1,090 °C

| Annealing time (h) → Temp. (°C) ↓ | Entity | 3 | 13 | 25 | 50 | 75 | 100 |
|---|---|---|---|---|---|---|---|
| 1060 | $Q$ (kJ/mol) | 228 ± 17 | 268 ± 24 | 306 ± 31 | 390 ± 42 | 419 ± 46 | 480 ± 68 |
| | $d$ (μm) | 0.1993 ± 0.014 | 0.3283 ± 0.028 | 0.3984 ± 0.04 | 0.4897 ± 0.052 | 0.5221 ± 0.056 | 0.5748 ± 0.081 |
| 1070 | $Q$ (kJ/mol) | 247 ± 17 | 291 ± 24 | 353 ± 43 | 458 ± 68 | 504 ± 74 | 550 ± 75 |
| | $d$ (μm) | 0.2133 ± 0.014 | 0.3542 ± 0.028 | 0.4337 ± 0.052 | 0.5496 ± 0.08 | 0.5914 ± 0.085 | 0.6574 ± 0.09 |
| 1090 | $Q$ (kJ/mol) | 283 ± 18 | 356 ± 27 | 420 ± 50 | 505 ± 74 | 544 ± 82 | 653 ± 103 |
| | $d$ (μm) | 0.2294 ± 0.015 | 0.3860 ± 0.03 | 0.4721 ± 0.055 | 0.6303 ± 0.092 | 0.7048 ± 0.1 | 0.8092 ± 0.13 |

as a constant in the present work, as in the previous one [3]. It should be pointed out here that several authors [12, 14, 15] indicate the intricate dependence of $k_0$ on the above variables, and long-term coarsening has been analyzed for evaluation of the rate constant or other parameters in several other alloys [for example, 16, 17]. Obviously, a more thorough analysis is warranted and will have to include any possible variations of the parameters involved in the rate constant.

Taking the precipitate size data obtained at any two of the given temperatures for a specific time interval and substituting them in the Eqs. 1 and 3 above, and assuming $d_0$ to be very small and negligible, one obtains:

$$Q = \frac{3R \ln\left(\frac{d_1}{d_2}\right)(T_1 T_2)}{T_1 - T_2} \tag{4}$$

where $d_1$ and $d_2$ are the average particle sizes at temperatures $T_1$ and $T_2$, respectively. The value of $Q$ obtained should prevail in the entire range between $T_1$ and $T_2$. Likewise, a value for $Q$ can be obtained for the continuing range $T_2$–$T_3$ from the data corresponding to the same time interval. One expects to get same $Q$ value if the activation energy does not change with increase in size of the precipitate particles. Results of the present study show that different values are obtained for the two ranges. Thus, one gets two values for the common temperature $T_2$, since different $Q$ values are obtained for the two ranges having $T_2$ as the common temperature. Therefore, the true value of activation energy corresponding to the common temperature $T_2$ should be a value between the two values obtained. In order to facilitate further analysis, the value of $Q$ obtained for any narrow temperature range is assigned for the mean temperature of the range. From the $Q$ value obtained and the values of $d_1$ and $d_2$ at temperatures $T_1$ and $T_2$ the corresponding $d$ value for the mean temperature $(T_1 + T_2)/2$ is calculated, and the $Q$ value obtained is taken to prevail at that size level calculated for the mean temperature. Similar procedure has been adopted in an earlier study on the activation energy for precipitate growth in the duplex size distribution as well [3].

Analysis of size data given for the different time intervals at the three different temperatures yields the values of activation energy $Q$ for the three mean temperatures of 1,060, 1,070, and 1,090 °C, corresponding to the different time intervals. The precipitate sizes corresponding to these mean temperatures and times have also been calculated. These are given in Table 2. Results from the previous work [2] yield the corresponding $Q$ and $d$ values from the 25-h annealing data at eight different temperatures in the range 850–1,120 °C. These are listed in Table 3. Finally, the activation energy for the growth of precipitate particles is plotted against the size of the particle incorporating all of the above results. Figure 4 gives this cumulative plot of $Q$ vs. '$d$'.

Data in Tables 2 and 3 as well as the plot in Fig. 4 clearly demonstrate that the activation energy for the growth of $\gamma'$ precipitate particles in IN738LC is not a

**Table 3** Activation energy $Q$ and the corresponding '$d$' values (average sizes) of precipitate particles after 25 h of annealing at the given temperatures [1, 2]

| Annealing temp. (°C) | Average precipitate sized $d$ (μm) | $Q$ (kJ/mol) |
|---|---|---|
| 850 | 0.112 −6/+10 | 162 ± 15 |
| 900 | 0.143 −10/+10 | 170 ± 15 |
| 950 | 0.187 −19/+10 | 187 ± 15 |
| 1000 | 0.222 −16/12 | 210 ± 16 |
| 1050 | 0.315 −14/+18 | 291 ± 24 |
| 1070 | 0.395 −25/+15 | 384 ± 40 |
| 1095 | 0.475 −25/+12 | 462 ± 70 |
| 1120 | 0.655 −25/+10 | 664 ± 110 |

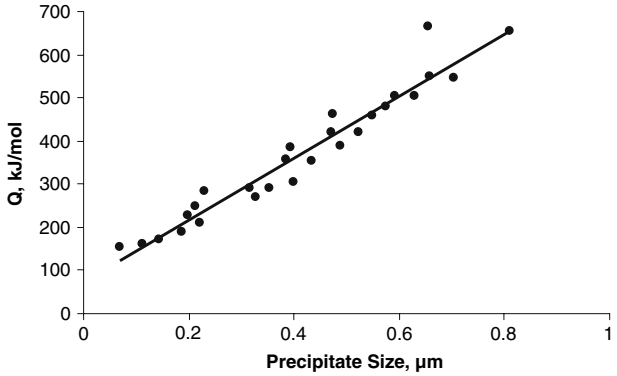


**Fig. 4** Figure plotting the data of activation energy '*Q*' vs. precipitate size at 1,060°, 1,070°, and 1,090 °C, together with the data from Balikci [1, 2] for lower temperatures, and the best linear fit for all the points

constant, but increases linearly with increasing size of the precipitates. This conclusion, already drawn in our earlier study [1, 2], is thus confirmed with a fairly large number of data points corresponding to different temperatures and times. Also, it can be pointed out that very good correlation seems to exist between the results of this study from the growth data at three different high temperatures in the range 1,000–1,100 °C for different annealing times and the results from the earlier study with the data from 25-h anneals involving analogous temperature range and several other lower temperatures, down to 850 °C, as well. All of the results obtained on precipitate growth in unimodal distribution of precipitates in IN738LC seem to indicate that the "pseudo-activation energy" continuously increases linearly with a constant rate.

Coarsening starts fast initially, but slows down as the growth continues, due to the reduction in the availability of the solute in the vicinity of the particles. The apparent activation energy needed for further growth seems to be enhanced too. As the precipitates grow coherently within the matrix by the Ostwald Ripening Mechanism (ORM), the overall surface energy will increase with increase in size of the particles and their elastic interactive energy with the matrix would build up in the lattice around the particles. Concurrently, a precipitate-denuded zone develops and the solute concentration decreases in the vicinity of the growing particles. Perhaps this leads to a zone-to-zone type diffusion with a reduced exponent '*n*', one for solute diffusion from the solute-depleted interface zone to the precipitate, as is pointed out by Ardell and Ozolins [18]. This or any other mechanism could be contributing to the steady increase in required activation energy for the growth of the particles. Thus the results of the present study seem to indicate the prevalence of different mechanisms of diffusion and/or different diffusion barriers contributing to the growth of precipitate particles in their unimodal distribution.

The steady linear increase in the activation energy seems to point to a steadily increasing resistance for solute atom diffusion. It is well known that as the particles grow, the misfit strain increases and this could be a contributing factor for the added diffusion barrier. The solute diffusion could proportionately require increasing activation energy, especially through the solute denuded interface zone. This is in contrast with the Particle Agglomeration Mechanism (PAM) which applies when two distinct and different precipitate size ranges are present (as in the duplex size precipitate microstructure), wherein the large-sized particles exert an attractive force on the much smaller ones and pull the latter toward them for coalescence [3]. The latter mechanism seems to prevail here whenever selected particles have grown to much larger sizes compared to the rest, as in the segregated duplex size precipitate distribution at much increased times, found in this study. The exact reasons for the apparent increase in the activation energy for diffusion-based growth of precipitates need to be enunciated further in future studies.

## Critical maximum sizes and dissolution features of precipitate particles

Particles located along the matrix grain boundaries tend to coarsen at a much faster pace than the rest. Such selected coarsening has been observed in samples annealed for longer time periods (>50 h) at 1,100 °C, Figs. 2d-right and 3. Such preferential coarsening occurring along the matrix grain boundaries implies easier growth conditions along the grain boundaries. The particle agglomeration mechanism seems to have prevailed also to some extent, since a

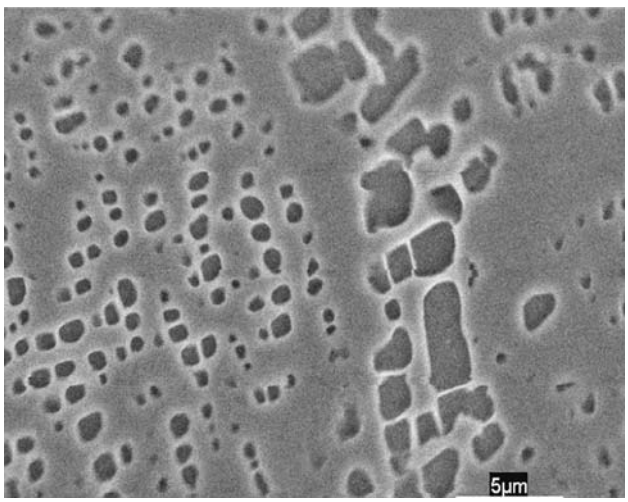


**Fig. 5** The micrograph showing coarse precipitates of more than 5.0 μm in size aligned in two layers along the grain boundary after annealing at 1,080 °C for 175 h (Magnification 3.5k×)

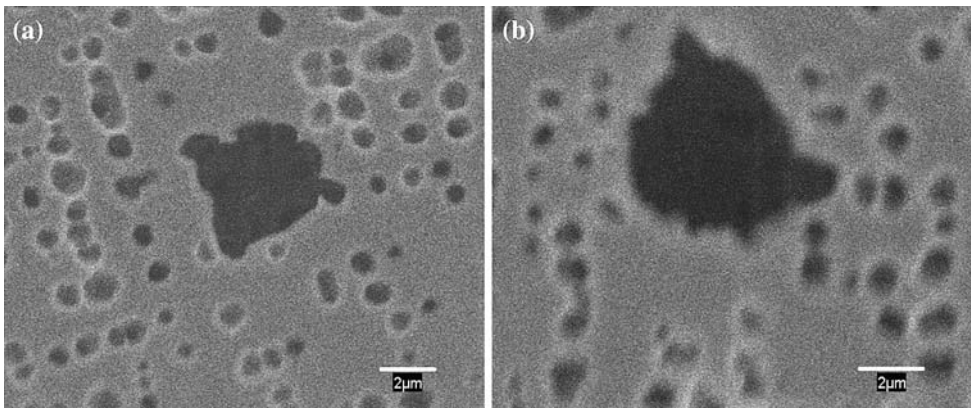


**Fig. 6** Microstructures with anomalous very coarse particle islands, not along grain boundary, after annealing at 1,100 °C for 200 h and water quenching. Magnification: 6k× (**a**) and 7k× (**b**). Average particle size: 4.5 μm (**a**) and 5.0 μm (**b**)

double layer of precipitates can be seen clearly along the grain boundaries in many instances and there also is a precipitate-denuded zone around such grain boundaries, see Figs. 3a, e and f and 5. Large-sized coarse particles, growing as isolated islands, are also seen, as in Fig. 6, though relatively sparsely. Merging of small particles with the coarse ones at their periphery is clearly illustrated in these cases. Such isolated islands of coarsening particles tend to acquire equiaxed or spheroidal morphology. On the contrary, although the PAM mechanism seems to be operative in the case of coarsening of particles lined along the grain boundaries, the particles tend to prefer a linear raft-like morphology there. This may be due to constraints based on the finite width of the grain boundary.

Many isolated very coarse $\gamma'$ particles with sizes larger than 4 μm were found after 200 h of holding at 1,100 °C. However, some among them were found to have grown to very large critical sizes. At this stage, when the critical maximum size is reached, the particles tend to break into smaller ones and/or dissolve. Four different modes of

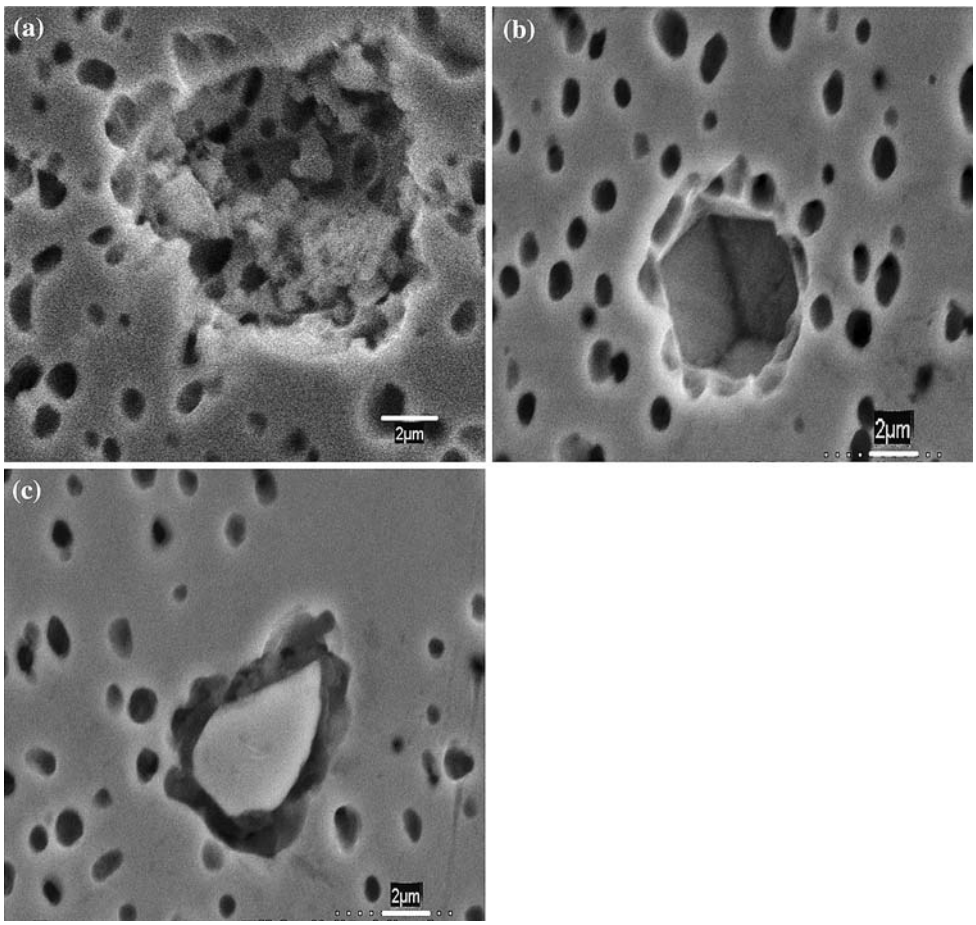


**Fig. 7** Micrographs showing Modes 1, 2, and 3 dissolutions of critical size precipitates in a specimen annealed at 1,100 °C for 200 h. (**a**) Mode 1. (**b**) Mode 2. (**c**) Mode 3

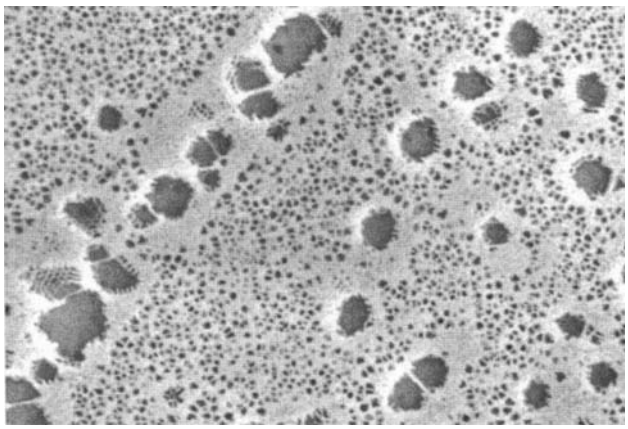

**Fig. 8** Figure showing splitting of critical coarse particles into two and subsequently to many fine fragments, lined probably along ⟨111⟩ directions, after annealing at 1,100 °C for 200 h starting from a duplex size precipitate microstructure. Note very coarse particles along grain boundaries and in isolated islands and fine precipitates all around. Magnification: 8k× [19]

dissolution of critical size particles have been seen in specimens annealed for 200 h at 1,100 °C. These are illustrated in Figs. 7 and 8 as Modes 1, 2, 3, and 4, respectively. In Mode 1, the coarsest critical precipitate seems to dissolve throughout on its surface by breaking into smaller fragments. The photomicrograph in Fig. 7a seems to indicate also that the coarse particle was not a single crystal, but a poly-grained aggregate which dissolved by breaking loose the smaller grains from the bulk particle. This is evident from the intergranular morphology of the dissolving surface and fine particles seen there on. In sharp contrast, the coarse particle in Fig. 7b appears to be an elongated cuboidal single crystal, at least at its central region, with well-developed flat facets, on which the dissolution seems to be taking place at its edge. This type of dissolution is denoted as Mode 2. In Mode 3, Fig. 7c, the dissolution seems to have started from its center and progressed toward the outer edges. This gives rise to a donut-shaped, partially dissolved coarsest critical particle and this type of dissolution can be occurring easily in relatively thin plate-type particles. It is felt that this type of dissolution is possible since the matrix and the precipitate have nearly similar lattice constants. In addition, a unique case where very coarse particles are splitting into a multitude of very fine particles lined along what appear to be the ⟨111⟩ directions is illustrated in Fig. 8. Such splitting in this case seems to be a prelude to the subsequent dissolution of the tiny particles after the splitting, Mode 4. Evidence for dissolution of several such split particles can be found in this photomicrograph as well. This photomicrograph also shows splitting of some coarse particles into two nearly equal grains with parallel boundary (see lower right and at the middle of the matrix grain boundary), prior to or concurrent with the break up of the critical particles into several smaller fragments at their edges. Thus, the given microstructure proves convincingly that more than eight fractions can form from one critical splitting particle.

It is known that coarse precipitates tend to split into smaller fractions to reduce the overall free energy of the system. Khachaturyan et al. [7] have given a theoretical analysis, modeling morphological transformations involving strain energies, and predict the splitting of particles after reaching a critical size. In several cases, the particles split into eight small cuboids or to a pair of parallel plates [4–7]. Dissolution along the edges of critical coarse grains by Mode 2 has already been reported in an earlier work from this group [8]. Likewise, dissolution of large particles through nucleation of the matrix phase at its center and by its growth toward the periphery is also reported in the literature [4, 9].

In the present case, dissolution was found to have started after the critical size of about 9–10 μm has been reached at 1,100 °C. It took nearly 200 h to reach this critical size. In earlier studies, Balikci has documented the edge-wise dissolution of coarse particles within the normal precipitate dissolution range at a temperature of 1,140 °C after reaching a critical size of about 0.3 μm in about 30 min. He also found a critical size for dissolution of about 2 μm at 1,120 °C, obtained after about 50 h [2].

It is known that even cooling precipitates of size as small as 70 nm (0.07 μm) would dissolve instantaneously (in less than one second) into the matrix when the material is heated at 1,160 °C [2, 8], whereas it is found to require about 200 h to reach the critical coarse size of about 9–10 μm at 1,100 °C, prior to dissolution. Thus, it is clear that for temperatures below 1,160 °C both the critical maximum size prior to dissolution and the time to reach the specific critical size would increase with decreasing temperature.

Data of approximate critical maximum sizes and the approximate times required to attain the criticality are given in Table 4. The data is plotted in Fig. 9. Using the results obtained from the temperatures in the range 1,160–1,100 °C, corresponding values for the temperatures 1,090 °C and 1,080 °C can be sought by extrapolation. The

**Table 4** Critical maximum sizes of $\gamma'$ particles and times required to attain those at different temperatures for onset of dissolution

| Temp. (°C) | Critical maximum $\gamma'$ size prior to dissolution (μm) | Approximate time required to attain maximum critical size (h) |
|---|---|---|
| 1160 | Below 0.07 | $<10^{-4}$ |
| 1140 | ~0.3 | 0.5 |
| 1120 | ~2 | 50 |
| 1100 | ~9 | 200 |

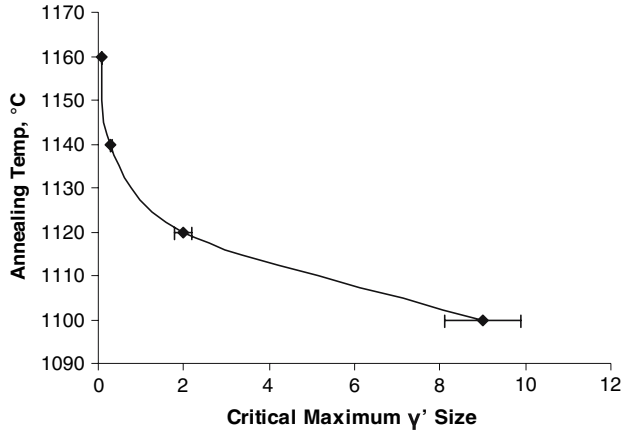


**Fig. 9** Plot of critical maximum size of $\gamma'$ (in μm) prior to dissolution vs. annealing temperature; includes data from Balikci [1, 2]

extrapolated critical sizes come out to be about 21 μm and 48 μm, respectively, and it would take about 37,198 h (4.25 years) and 534,988 h (61 years), respectively, at these two temperatures. These times, required to reach critical coarse sizes prior to dissolution, are so large and beyond the normal time periods in use that one can infer that the precipitates would not grow to critical coarse sizes and split or dissolve during practical applications at temperatures below about 1,100 °C in the superalloy IN738LC. However, continuous coarsening at such high temperatures would still be possible and be of concern, as it would adversely affect the mechanical properties, particularly the creep resistance and stress rupture characteristics at high temperatures.

Although the splitting of coarsest particles of critical sizes can be understood as due to the need for reduction in surface strain energy, the reasons for dissolution of such critical particles cannot be understood. Since at a given temperature, under equilibrium conditions, the volume fraction of the precipitate phase can be expected to remain constant and dissolution would reduce the volume fraction, the dissolved solute can be expected to lead to reprecipitation. The dissolution and reprecipitation in the vicinity could be to eliminate the dislocation networks present around the precipitates and obtain dislocation (strain)-free fine precipitates. The presence of fine precipitates in the entire bulk in the 200 h annealed sample in Fig. 8 seems to support this view. Hence, what happens after dissolution at such high temperatures during prolonged exposures needs to be studied further. Indeed, if strain-free fine particles were formed, since they would begin to grow further if kept for longer periods of time, it can be suggested that they would grow to critical sizes again, perhaps after another 200 h at 1,100 °C, and the process itself could repeat. This possibility is under further investigation.

**Acknowledgement** The authors acknowledge partial support for supplies from the NASA LASPACE Grant NASA (00-01)—DGAP-08, given through LA-EPSCOR.

## References

1. Balikci E, Raman A, Mirshams RA (1997) Met Mater Trans A 28A:1993
2. Balikci E (1998) Ph.D. Dissertation, Louisiana State University, Baton Rouge, LA, USA
3. Roy I, Balikci E, Ibekwe S, Raman A (2005) J Mater Sci 40(23):6207
4. Miyazaki T, Imamura M, Kozakai T (1982) Mater Sci Eng 54:9
5. Doi M, Miyazaki T, Wakatsuki T (1984) Mater Sci Eng 67:247
6. Yeom SJ, Yoon DY, Henry MF (1993) Met Trans A 24A:1975; see also references 14 to 19 given in that work for prior observation of octets
7. Khachaturyan AG, Semenovskaya SV, Morris JW Jr (1988) Acta Met 36(6):1563
8. Balikci E, Mirshams RA, Raman A (1999) Z Metallkd 90:132
9. Mughrabi H, Tetzlaff U (2000) Adv Eng Mater 2(6):319
10. Lifshitz I, Slyozov V (1961) J Phys Chem Solids 11:35
11. Wagner C (1961) Z Electrochem 65:581
12. Baldan A (2002) J Mater Sci 37(12):2391
13. Balikci E, Ferrell RE Jr, Raman A (1999) Z Metallkd 90:141
14. Kuehmann CJ, Voorhees PW (1996) Met Mater Trans 27A:937
15. Snyder VA, Alkemper J, Voorhees PW (2001) Acta Mater 49:699
16. Footner PK, Richards BP (1982) J Mater Sci 17(7):2141
17. Ges A, Fornaro O, Palacio H (1997) J Mater Sci 32(14):3687
18. Ardell AJ, Ozolins V (2005) Nat Mater 4:309
19. Roy I (2003) M.S. Thesis, Louisiana State University, Baton Rouge, LA, USA